



Short communication

High-efficiency carbon-supported platinum catalysts stabilized with sodium citrate for methanol oxidation

Zhengyu Bai^a, Lin Yang^{a,*}, Jiangshan Zhang^b, Lei Li^c, Chuangang Hu^a, Jing Lv^a, Yuming Guo^a^a College of Chemistry and Environmental Science, Henan Normal University, 46# East of Construction Road, Xinxiang 453007, China^b College of Chemistry and Chemical Engineering, Anyang Normal University, Anyang 455002, China^c School of Chemistry and Chemical Technology, Shanghai Jiao Tong University, Shanghai 200240, China

ARTICLE INFO

Article history:

Received 28 July 2009

Received in revised form

14 September 2009

Accepted 2 November 2009

Available online 6 November 2009

Keywords:

Methanol oxidation

Active metal

Platinum

Electrocatalysis

Sodium citrate

ABSTRACT

A high-efficiency platinum catalyst stabilized with sodium citrate for methanol oxidation is introduced in this paper, in which freshly prepared non-noble active cobalt is employed as reducer. According to X-ray diffraction (XRD) and transmission electron microscopy (TEM) measurements, the novel as-prepared nanoclusters Pt catalyst dispersed on carbon is composed of Pt nanoparticles, and the average particle size of the Pt nanoparticles is 2.0 nm. The catalyst with sodium citrate shows a very high electrochemically active surface area and significant increase electrocatalytic activity towards methanol oxidation, which indicates that it would be a better potential candidate for application in a direct methanol fuel cell (DMFC).

© 2009 Elsevier B.V. All rights reserved.

1. Introduction

Direct methanol fuel cell (DMFC) has attracted tremendous attention because the direct-fed liquid fuel cells are perfect for portable power and mobile applications due to the high energy density, compact system and low operating temperatures [1–5]. However, high cost of catalysts caused by the exclusive use of platinum and platinum-based catalysts in the fuel-cell electrodes is one of the major barriers to limit the commercial application of DMFCs. In order to reduce the cost of catalysts, on the one hand, less expensive, more abundant non-platinum catalysts have been widely studied [6–8], however, their catalytic activities, stabilities, and utility efficiencies should be further improved. On the other hand, many efforts in this field have been devoted to further improve the utility efficiencies of platinum catalysts [9–11], because of excellent catalytic activity of Pt and Pt-based for DMFCs involving methanol oxidation and oxygen reduction in acidic solution. Enlarging electrochemical active surface (EAS) through adjusting the size and shape has been viewed as a major strategy to improve the utility efficiencies, which has involved the utilization of the relatively weak reductant [12,13] and the use of surface modification with

surfactants [14] and polymers [15,16] as stabilizing agents. Dong et al. reported the preparation of Pt nanostructures with urchin-like morphology in the presence of poly(vinyl pyrrolidone) (PVP) [17]. Li and his coworkers prepared Pt/XC-72 catalyst and studied the effect of naphthalene sulfonic acid as dopant on the electrochemical oxidation of hydrogen and methanol [18]. Pd/PPy-XC-72 catalyst with hollow nanospheric Pd entrapped in the structure of PPy was prepared *via* a very simple chemical reduction method in our previous study [19].

In this paper, we present one new synthetic route to prepare the Pt nanoparticles with small particle size. In the present work, sodium citrate was used as stabilizer, and freshly prepared active cobalt was employed as reducing agent, then platinum nanoclusters composed of nanoparticles with particle size smaller than 3 nm were prepared through the replacement reaction. Sodium citrate is one of the most commonly used agents in the synthesis of metallic and semiconductor nanoparticles because it can act as a coordination agent. Many metal nanoparticles (such as Pd, Co) [20,21] with small particle size have been synthesized in the presence of sodium citrate. Furthermore, freshly prepared cobalt nanoparticle has a poorer reducing power compared with KBH₄, and it may also contribute to the synthesis of smaller Pt nanoparticles. Attributing to the enhanced dispersivity and stability in the presence of citrate anion and freshly prepared cobalt nanoparticles, the as-prepared catalyst showed very small particle size and high EAS, and then the electrocatalytic activity increased significantly.

* Corresponding author. Tel.: +86 373 3328117; fax: +86 373 3328507.
E-mail address: yanglin1819@163.com (L. Yang).

2. Experimental

2.1. Materials

Sodium citrate, potassium borohydride (KBH_4) and $\text{Co}(\text{NO}_3)_2 \cdot 6\text{H}_2\text{O}$ were obtained from China National Pharmaceutical Group Corp., and catalyst precursor salt $\text{H}_2\text{PtCl}_6 \cdot 6\text{H}_2\text{O}$ was purchased from Alfa Aesar. Double distilled water (DD water) was used throughout the experiments. Vulcan XC-72 carbon powder from Cabot Company was pre-treated with 6 M HNO_3 at 100°C for 8 h, subsequently washed with DD water and dried at room temperature under vacuum condition for 24 h.

2.2. Preparation of Pt/XC-72 catalyst

2.2.1. Typical preparation of Pt/XC-72 catalyst with sodium citrate as stabilizer

Eighty milligrams pre-treated XC-72, 217 mg $\text{Co}(\text{NO}_3)_2 \cdot 6\text{H}_2\text{O}$ and 100 mg sodium citrate were added in 100 mL ethanol–water (1:1, v/v) solution, and ultrasonically treated for 30 min, then purged with N_2 under stirring for 1 h to keep the saturation N_2 atmosphere. A freshly prepared KBH_4 solution (100 mg in 100 mL DD water) was added dropwise into the above solution under stirring for 2 h to form Co nanocrystals, and then the stirring was continued for another 10 h to make sure the completely decomposition of the redundant KBH_4 . Afterwards, a precursor aqueous solution with right amount H_2PtCl_6 was added dropwise into the suspension with vigorously stirring for 5 h. The whole process was operated at room temperature. Finally, the product was collected by filtration and washed several times with DD water and ethanol, then dried at 40°C in vacuum condition for 12 h.

2.2.2. Control experiment A: preparation of Pt/XC-72 catalyst with KBH_4 as reducing agent directly rather than precursor Co nanoparticles

Eighty milligrams pre-treated XC-72, 100 mg sodium citrate and a precursor aqueous solution with right amount H_2PtCl_6 were added in 100 mL ethanol–water (1:1, v/v) solution, and ultrasonically treated for 30 min, then kept stirring for 1 h. A freshly prepared solution of KBH_4 (100 mg in 100 mL DD water) was added dropwise into the above solution under stirring for 2 h to form Pt nanocrystals, and then the stirring was continued for another 10 h to make sure the completely decomposition of the redundant KBH_4 . Finally, the product was collected by filtration and washed several times with DD water and ethanol, then dried at 40°C in vacuum condition for 12 h.

2.2.3. Control experiment B: the preparation of Pt/XC-72 catalyst without sodium citrate as stabilizer

Control B was done in the same conditions described as the typical experiment, apart from the sodium citrate as stabilizer.

2.3. Fabrication of 20% Pt/XC-72 electrodes

Catalyst ink was prepared by blending 20 wt% Pt/XC-72 catalyst with ethanol and 5 wt% perfluorosulfonic acid (PFSA) ionomer solution (Dongyue Group Co. Ltd., China). Five milligrams catalyst was added into 0.5 mL ethanol and 50 μL of 5 wt% PFSA solution, and ultrasonically mixed for 3 min. Then, 15 μL mixed solution was uniformly dispersed on glassy carbon electrode and dried at room temperature.

2.4. Measurements

The morphology of catalyst was measured by JEOL-100CX high resolution transmission electron microscopy (HRTEM) operated

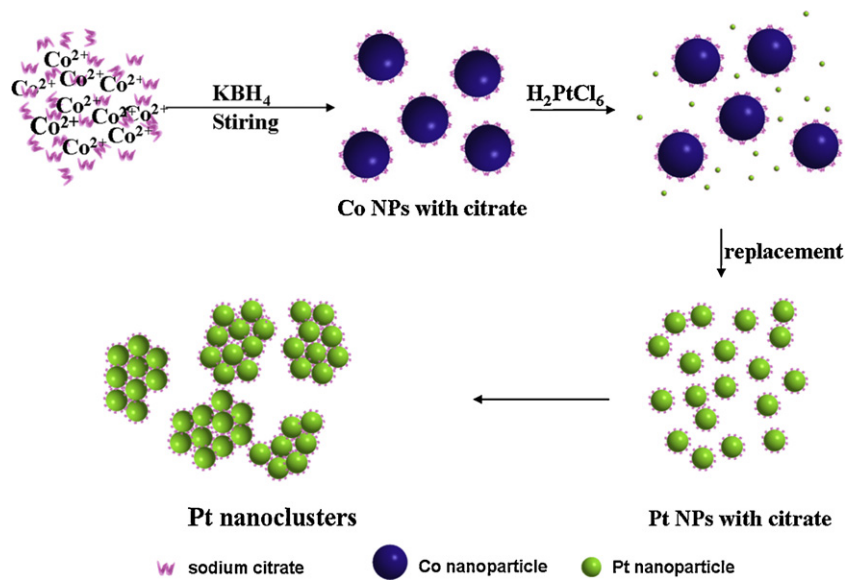
at 200 kV. Nanoparticles were firstly immersed into ethanol and subsequently dispersed ultrasonically for 5 min. A drop of the suspension was then deposited on a lacey carbon grid and dried in air for TEM observations. Powder X-ray diffraction (XRD) pattern was investigated using D/max-2200/PC X-ray diffractometer with $\text{Cu K}\alpha$ radiation source. The Fourier transform infrared spectroscopy (FT-IR) spectra were recorded on a Bio-Rad FTS-40 Fourier transform infrared spectrometer in the wavenumber range of $4000\text{--}400\text{ cm}^{-1}$, and the thermogravimetric analysis (TGA) were performed on a NETZSCH STA 449C instrument.

Cyclic voltammetry measurements were carried out in a three-electrode cell by using Solartron 1287 electrochemical test system (Solartron Analytical, England). A glassy carbon disk (3 mm o.d.) coated with catalyst was used as the working electrode, a platinum foil (1 cm^{-2}) as the counter-electrode, and an Ag/AgCl electrode as the reference. 0.5 M H_2SO_4 aqueous solution was served as the electrolyte for hydrogen oxidation measurements, and 0.5 M CH_3OH in 0.5 M H_2SO_4 for methanol oxidation measurements, respectively. High-purity N_2 was bubbled into the electrolytes during the experiments.

3. Results and discussion

In this work, a two-step strategy was employed, named the generation of active cobalt–carbon composite and the formation of Pt nanocluster catalysts. The Pt nanocluster catalysts were prepared through the surface replacement reaction, which was supported by Vulcan XC-72 carbon powders. The formation mechanism of Pt nanocluster catalysts may be as follows (shown in Scheme 1.). Firstly, the cobalt source Co^{2+} was mixed with sodium citrate which was used as the coordination agent, and then the Co^{2+} was reduced to Co nanoparticles with KBH_4 as the reducing agent. Secondly, freshly prepared active cobalt was employed as the reducer, and the Pt/XC-72 nanoparticles were formed through adding H_2PtCl_6 . Finally, the Pt nanoclusters were formed in the presence of sodium citrate as stabilizer.

Fig. 1 shows transmission electron microscopy (TEM) images of the resulting samples from typical and control experiments, and their size frequency curves. From Fig. 1a, the final product from typical experiment, Pt nanoclusters composed of nanoparticles with a smaller particle size is well-dispersed on the surface of Vulcan XC-72 carbon support. The nanoparticles diameters obtained from the HRTEM image (inset in Fig. 1b) range from 1.1 to 3.2 nm and the mean size calculated by the Gauss distribution is 2.0 nm (see Fig. 1b). To investigate the influence of active metal cobalt and sodium citrate on the formation of the Pt nanoparticles, two sets of control experiments were carried out. Control A was done with KBH_4 as reducer in the absence of active metal cobalt (see Fig. 1c), in which Pt nanoclusters composed of nanoparticles were also formed, but the mean size of 3.6 nm was larger than that of the typical experiment. The result shows that the freshly prepared active cobalt employed as reducer is important in regulating the size of the Pt nanoparticles. To further study the effect of sodium citrate, control B was done in the same conditions described as the typical experiment, apart from the sodium citrate as dispersant and stabilizer, while carbon-supported Pt nanoparticles with a much larger size were formed with serious agglomeration (see Fig. 1d). The results demonstrate that the presence of sodium citrate is a key factor in controlling the size of the Pt nanoparticles. The stabilizing property of sodium citrate may be rendered by its three carboxyl anions. During the reaction process, the three carboxyl anions maybe adsorb the metal particles and stabilize them, then prevent them from growth and agglomeration. At the same time, freshly prepared active metal cobalt has a poorer reducing power compared with KBH_4 , so that Pt nanoparticles come into being in



Scheme 1. Formation mechanism of Pt nanocluster catalyst.

a slower speed. In addition, it may also contribute to the synthesis of Pt nanoparticles with a small particle size.

Fig. 2a and b shows the XRD patterns of the as-prepared Pt/XC-72 composite catalysts with and without sodium citrate, respectively. It can be observed from the XRD patterns that four

peaks at 39.8°, 46.3°, 67.6°, 81.9° are characteristics of face-centered-cubic (fcc) crystalline Pt, which are corresponding to the facets (111), (200), (220) and (311), respectively, except for the characteristic peak of amorphous Vulcan XC-72 carbon support at 24.5°. Furthermore, no peaks related to Co are observed,

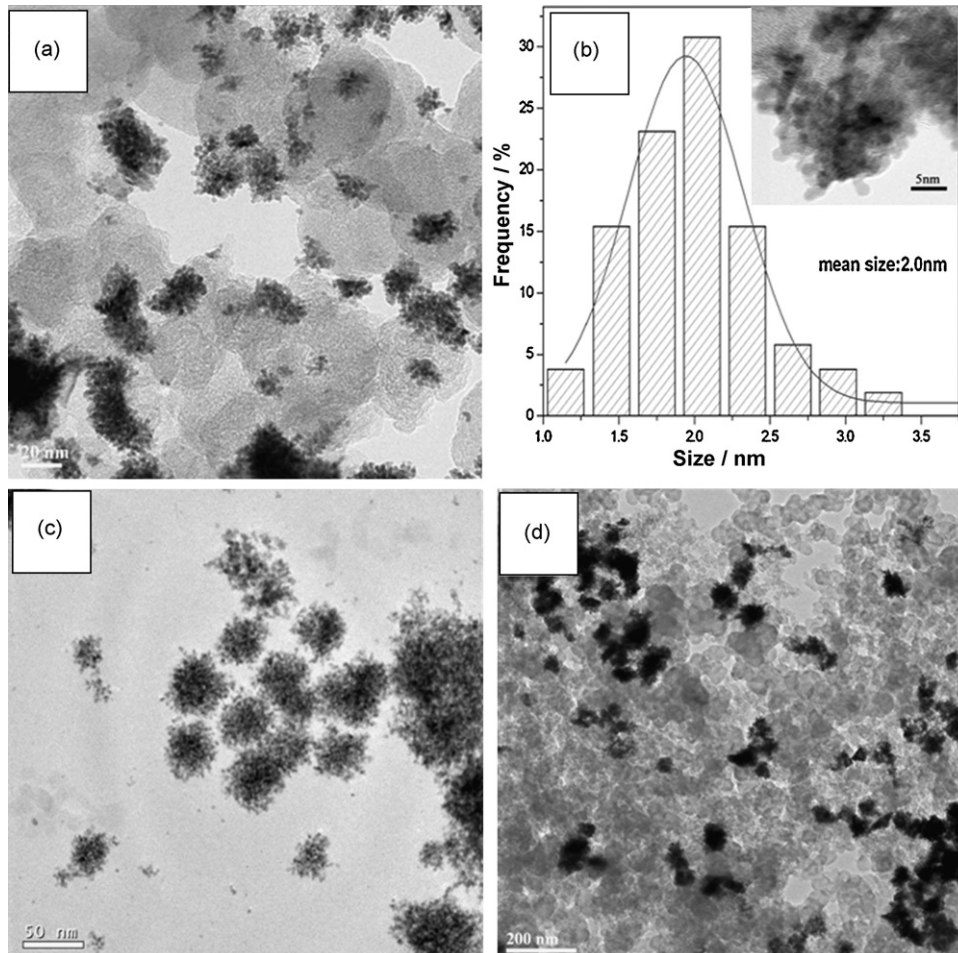


Fig. 1. TEM images of the Pt/XC-72 catalysts from (a) the typical experiment, (b) its size frequency curve, (c) control A experiment, and (d) control B experiment.

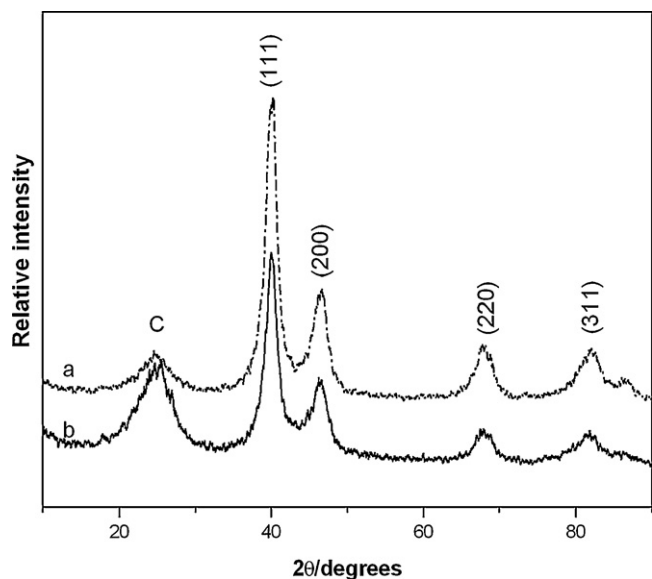


Fig. 2. X-ray diffraction patterns of the as-prepared Pt/XC-72 composite catalysts with (a) and without (b) sodium citrate.

demonstrating that cobalt has been redissolved into solution by the replacement reaction. From the X-ray diffraction pattern in Fig. 2, it can be also observed that the full width at half maximum (FWHM) of the diffraction peak in radians of the catalyst with sodium citrate is wider than that of the catalyst without sodium citrate. The wider the FWHM, the smaller particle size is. This result is in accordance with the HRTEM image.

In order to confirm the existence of sodium citrate, the Pt/XC-72 composite was characterized by FT-IR and TGA. Fig. 3 shows the FT-IR spectra of sodium citrate and as-prepared Pt catalyst with sodium citrate. The pure sodium citrate is characterized by major peaks at 1594 and 1419 cm^{-1} assigned to the unsymmetrical stretching vibration and stretching vibration of COO^- , and at 3454 and 3268 cm^{-1} to the stretching vibration of $-\text{OH}$ in sodium citrate and $-\text{OH}$ of the crystal water, respectively [22]. As shown in Fig. 3a, the FT-IR spectrum of as-prepared Pt catalyst with sodium citrate is different from that of the pure sodium citrate. Compared with pure sodium citrate, the peaks at 1594 and 1419 cm^{-1} shifted to 1572

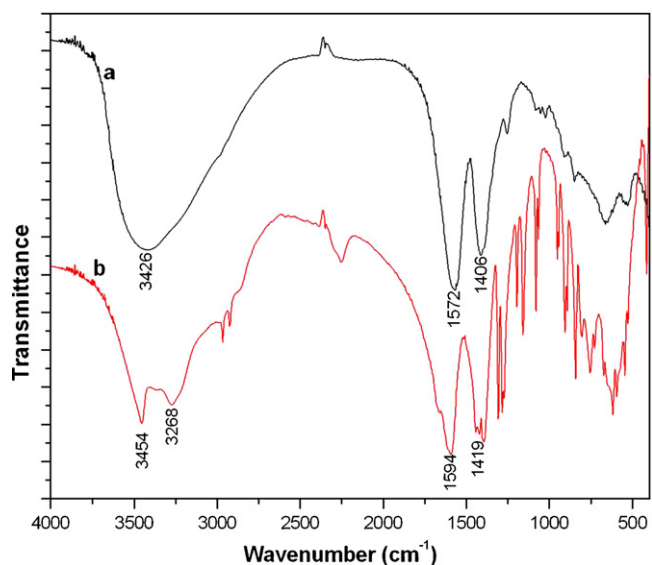


Fig. 3. FT-IR spectra of the samples: (a) the as-prepared Pt/XC-72 catalysts with sodium citrate and (b) pure sodium citrate.

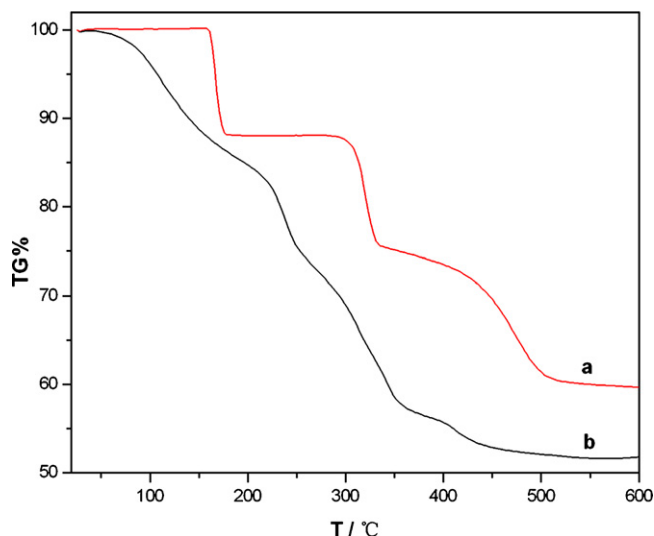


Fig. 4. TGA curves of (a) sodium citrate and (b) the as-prepared Pt/XC-72 catalysts with sodium citrate, both of them were under the protection of N_2 .

and 1406 cm^{-1} , the band at 3454 cm^{-1} shifted to low wavenumber, and then overlapped with the band at 3268 cm^{-1} into one band at 3426 cm^{-1} . These may due to the presence of the Pt atoms, suggesting that there might be coordination interaction between Pt and COO^- , $-\text{OH}$ of citrate. Overall, these FT-IR spectra show that Pt atoms are modified by sodium citrate. The TGA curves shown in Fig. 4 compare the thermal-decomposition curves of pure sodium citrate with two crystal water and as-prepared Pt catalyst with sodium citrate under the protection of N_2 at a heating rate of 10°min^{-1} from 50 to 600 °C. For the TGA curve of pure sodium citrate, there are three stages of weight loss. The weight loss with about 12 wt% in the first stage around 170 °C is attributed to the loss of the crystal water. The second stage, which starts at around 300 °C, corresponds to the partially degradation of the sodium citrate. The last stage is from 400 to 500 °C, owing to the decomposition of the residues. The as-prepared Pt catalyst with sodium citrate shows an earlier initial weight loss and the faster weight loss, as compared to the pure sodium citrate. The TGA data suggest that decomposition of the composite appears to be activated in the presence of Pt [15].

Fig. 5 compares the electrochemical reactivity and electrochemically active surface areas of different catalysts determined by cyclic voltammetry measurement performed in 0.5 M H_2SO_4 electrolyte at a scan rate of 50 mV s^{-1} . In Fig. 5, cyclic voltammograms of the samples belong to the typical experiment, two control experiments, and a commercial 40% Pt/C catalyst. As shown in Fig. 5, the hydrogen adsorption peak of Pt/XC-72 catalyst from the typical experiment is much larger than the others. According to the coulombic amount (Q) associated with the peak area, the EAS area can be calculated using the following equation [23,24]:

$$\text{EAS} = \frac{Q}{mC}$$

where C denotes the quantity of electricity when hydrogen molecules are adsorbed on platinum with a homogenous and single layer, here it is $210 \mu\text{C cm}^2$, m is the mass of platinum on catalyst surface.

The EAS value of Pt/XC-72 catalyst from the typical experiment is the largest among two control experiments, and a commercial 40 wt% Pt/C catalyst (shown in Table 1), indicating an enhanced electrochemical activity with sodium citrate compared to the others. It demonstrates that the presence of sodium citrate and freshly prepared active cobalt both may be important factors for the significant improvement in the electrochemical performance.

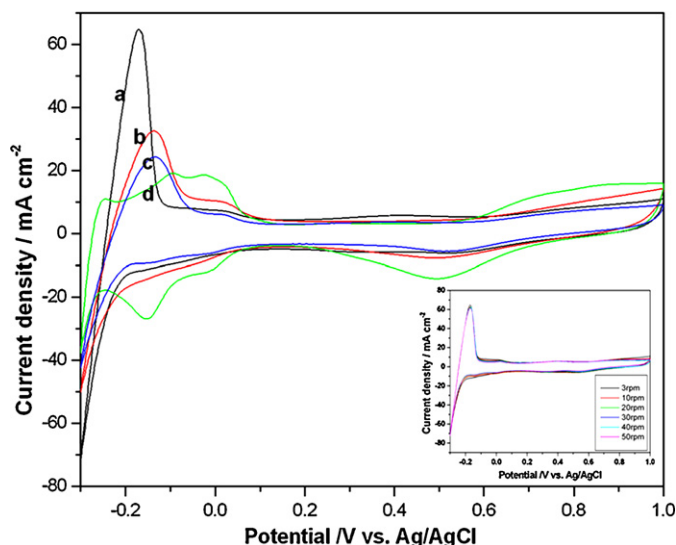


Fig. 5. Cyclic voltammograms of Pt/XC-72 catalysts from (a) the typical experiment, (b) control A experiment, (c) control B experiment, and (d) a commercial 40% Pt/C catalyst on glassy carbon electrode, electrolyte: 0.5 M H_2SO_4 aqueous solution, sweep rate of 50 mV s^{-1} , at 25°C .

Table 1

Electrochemical active surface of different catalysts.

Catalyst	Typical experiment	Control A	Control B	Commercial 40% Pt/C
EAS ($\text{m}^2 \text{g}^{-1} \text{ Pt/Pd}$)	102	68	59	62

The electrochemical stability of the as-prepared Pt/XC-72 catalyst from the typical experiment was further studied by an additional CV experiment in H_2SO_4 aqueous solution (inset in Fig. 5). It shows excellent stability during cycling according to the curves. In the CV curves, there is almost no drop in the peak current density after 50 cycles cyclic voltammetry measurement process.

Fig. 6 is a comparison of methanol oxidation on catalysts from the typical experiment, two control experiments, and a commercial 40% Pt/C catalyst, which is tested in 0.5 M $\text{H}_2\text{SO}_4 + 0.5 \text{ M CH}_3\text{OH}$

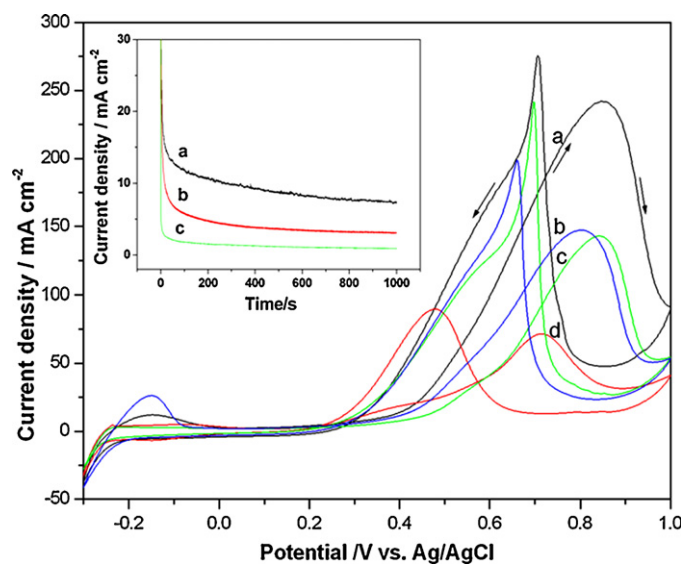


Fig. 6. Cyclic voltammograms and corresponding chronoamperometry curves of Pt/XC-72 from (a) the typical experiment, (b) control A experiment, (c) control B experiment, and (d) a commercial 40% Pt/C catalyst on glassy carbon electrode, electrolyte: 0.5 M $\text{H}_2\text{SO}_4 + 0.5 \text{ M CH}_2\text{OH}$ aqueous solution, sweep rate of 50 mV s^{-1} , at 25°C .

aqueous solution under half-cell condition. From the curves, two main peaks for the methanol oxidation in both positive and negative scan direction are observed, and the corresponding peak current densities are both over 140 mA cm^{-2} , which are much higher than the commercial 40% Pt/C catalyst. It can be seen clearly that the peak current densities of the as-prepared Pt/XC-72 catalysts are much higher than those of others. In order to compare the electrochemical stability of the as-prepared three Pt/XC-72 catalysts towards the methanol oxidation reaction, chronoamperometry tests were carried out in 0.5 M $\text{H}_2\text{SO}_4 + 0.5 \text{ M CH}_3\text{OH}$ aqueous solution at 0.5 V for 1000 s (inset in Fig. 6). Obviously, the current of typical preparation of Pt/XC-72 for methanol oxidation remains higher than the other catalysts, which indicate that the Pt/XC-72 with sodium citrate and freshly prepared active cobalt has the better catalytic activity for methanol oxidation and the higher stability. This result is in agreement with those of the cyclic voltamograms measurement. And it also suggests that the existence of freshly prepared active cobalt and sodium citrate in catalyst is important to the electrocatalytic activities. In addition, the beginning potential of the reaction current with the as-prepared catalysts is a little higher than that of the commercial sample. It may be brought by the changes in the relative intensity of planes, which the (2 0 0) and (1 1 1) diffraction peaks are much stronger, while the (3 1 1) diffraction peak becomes weaker obviously. Similar results have been reported in previous study [25].

4. Conclusions

In conclusion, a high-efficiency platinum catalyst with sodium citrate for methanol oxidation stabilized was prepared at room temperature. Herein, dispersivity and the ESA of the Pt nanoclusters enhanced obviously in the presence of freshly prepared active cobalt employed as reducer and sodium citrate as stabilizer, and then the electrocatalytic activity and utilization ratio of the catalyst increased significantly.

The electrocatalytic activity of the as-prepared Pt/XC-72 catalyst with sodium citrate for methanol oxidation is much higher than those of without sodium citrate and commercial 40% Pt/C. The nanoclusters structure enlarged the EAS of catalysts through the direct pathway, so that enhanced the electrocatalytic activity.

Acknowledgment

This work was financially supported by the National Key Basic Research and Development Program of China (Grant No. 2009CB626610), the National Science Foundation of China (Grant No. 20771036), the National Research Fund for the Doctoral Program of Higher Education of China (Grant No. 20070476001), and Henan Key Proposed Program for Basic and Frontier Research (Grant No. 092300410121).

References

- [1] S. Wadmus, A. Küver, *Electrochem. Commun.* 461 (1999) 14.
- [2] V.M. Barragan, A. Heinzl, *J. Power Sources* 104 (2002) 66–72.
- [3] E. Antolini, E.R. Gonzalez, J.R.C. Salgado, *Appl. Catal. B: Environ.* 63 (2006) 137.
- [4] C. Lamy, A. Lima, V. Le Rhun, C. Coutanceau, J.M. Leger, *J. Power Sources* 105 (2002) 283.
- [5] E. Reddington, A. Sapienza, B. Gurau, R. Viswanathan, S. Sarangapani, E.S. Smotkin, T.E. Mallouk, *Science* 280 (1998) 1735.
- [6] Y.M. Zhu, Z. Khana, R.I. Masela, *J. Power Sources* 139 (2005) 15.
- [7] R.S. Jayashree, J.S. Spindelov, J. Yeom, C. Rastogi, M.A. Shannon, P.J.A. Kenis, *Electrochim. Acta* 50 (2005) 4674.
- [8] X.G. Li, I.M. Hsing, *Electrochim. Acta* 51 (2006) 3477.
- [9] V. Selvaraj, M. Alagar, *Electrochem. Commun.* 9 (2007) 1145.
- [10] K. Wikander, H. Ekström, A.E.C. Palmqvist, G. Lindbergh, *Electrochim. Acta* 52 (2007) 6848.
- [11] G.A. Camara, E.A. Ticianelli, S. Mukerjee, S.J. Lee, J. McBreen, *J. Electrochem. Soc.* 149 (2002) A748.

- [12] Z.H. Wen, J. Liu, J.H. Li, *Adv. Mater.* 20 (2008) 743–747.
- [13] S.H. Sun, F. Jaouen, J.P. Dodelet, *Adv. Mater.* 20 (2008) 3900–3904.
- [14] Y.S. Kim, H.J. Kim, W.B. Kim, *Electrochem. Commun.* 11 (2009) 1026–1029.
- [15] B. Rajesh, Z. Piotr, *Nature* 443 (2006) 63–71.
- [16] W. Martínez Millán, T. Toledano Thompson, L.G. Arriaga, M.A. Smit, *Int. J. Hydrogen Energy* 34 (2009) 694–702.
- [17] L. Wang, S.J. Guo, J.F. Zhai, S.J. Dong, *J. Phys. Chem. C* 112 (2008) 13372–13377.
- [18] H.B. Zhao, L. Li, J. Yang, Y.M. Zhang, *J. Power Sources* 184 (2008) 375–380.
- [19] Z.Y. Bai, L. Yang, L. Li, J. Lv, K. Wang, J. Zhang, *J. Phys. Chem. C* 113 (2009) 10568–10573.
- [20] J.J. Ge, W. Xing, X.Z. Xue, C.P. Liu, *J. Phys. Chem. C* 111 (2007) 17305–17310.
- [21] R.F. Wang, S.J. Liao, S. Ji, *J. Power Sources* 180 (2008) 205–208.
- [22] J. Tronto, M.J. dos Reis, F. Silveirio, V.R. Balbo, J.M. Marchetti, J. Valim, *J. Phys. Chem. Solids* 65 (2004) 475–480.
- [23] J. Fournier, G. Fuabert, J.Y. Tilquin, *J. Electrochem. Soc.* 144 (1997) 145–154.
- [24] K.W. Park, J.H. Choi, K.S. Ahn, *J. Phys. Chem. B* 108 (2004) 5989–5994.
- [25] D. Xu, Z.P. Liu, H.Z. Yang, Q.S. Liu, J. Zhang, J.Y. Fang, S.Z. Zou, K. Sun, *Angew. Chem. Int. Ed.* 48 (2009) 4217–4221.